Experimental and Theoretical Studies on DNA-Binding and Spectral Properties of 'Light Switch' Complexes $[Ru(L)_2(ppn)]^{2+}$ (L = 2,2′-Bipyridine and 1,10-Phenanthroline; ppn = Pteridino[6,7-*f*][1,10]phenanthroline-11,13-diamine)

by **Xue-Wen Liu**[a])[b]), **Jin-Can Chen**[a]), **Xia Hu**[b]), **Hong Li**[c]), **Kang-Cheng Zheng***[a]), and **Liang-Nian Ji***[a])

[a]) The Key Laboratory of Bioinorganic and Synthetic Chemistry of Ministry of Education/School of Chemistry and Chemical Engineering, Sun Yat-Sen University, Guangzhou 510275, P. R. China (phone: +86-20-84110696; fax: +86-20-84112245; e-mail: ceszkc@mail.sysu.edu.cn (*K.-C. Z.*), cesjln@mail.sysu.edu.cn (*L.-N. J.*))

[b]) Department of Chemistry and Chemical Engineering, Hunan University of Arts and Science, ChangDe 415000, P. R. China

[c]) Department of Chemistry, Southern China Normal University, Guangzhou 510000, P. R. China

The ligand pteridino[6,7-*f*][1,10]phenanthroline-11,13-diamine (ppn) and its Ru^{II} complexes $[Ru(bpy)_2(ppn)]^{2+}$ (**1**; bpy = 2,2′-bipyridine) and $[Ru(phen)_2(ppn)]^{2+}$ (**2**; phen = 1,10-phenanthroline) were synthesized and characterized by elemental analysis, electrospray MS, ^{1}H-NMR, and cyclic voltammetry. The DNA-binding behaviors of **1** and **2** were studied by spectroscopic and viscosity measurements. The results indicate that both complexes strongly bind to calf-thymus DNA in an intercalative mode, with DNA-binding constants K_b of $(1.7 \pm 0.4) \cdot 10^6$ M^{-1} and $(2.6 \pm 0.2) \cdot 10^6$ M^{-1}, respectively. The complexes **1** and **2** exhibit excellent DNA-'light switch' performances, *i.e.*, they do not (or extremely weakly) show luminescence in aqueous solution at room temperature but are strongly luminescent in the presence of DNA. In particular, the experimental results suggest that the ancillary ligands bpy and phen not only have a significant effect on the DNA-binding affinities of **1** and **2** but also have a certain effect on their spectral properties. $[Ru(phen)_2(ppn)]^{2+}$(**2**) might be developed into a very prospective DNA-'light switch' complex. To explain the DNA-binding and spectral properties of **1** and **2**, theoretical calculations were also carried out applying the DFT/TDDFT method.

1. Introduction. – The DNA-binding and spectral properties of transition-metal complexes have captured an extensive interest over the past decades because these properties are closely related to their potential applications, *e.g.*, DNA molecular 'light switches', chemical and stereoselective probes of DNA structures, as well as possible antitumor agents, *etc.* [1–3]. In particular, Ru^{II} complexes with polypyridine ligands, due to a combination of easily constructed rigid chiral structures spanning all three dimensions and a rich photophysical repertoire, have attracted considerable attention [2–7]. These Ru^{II} complexes can bind to DNA in a noncovalent interaction such as electrostatic binding, groove binding, or intercalation. Many important applications of these complexes require that the complexes could bind to DNA in an intercalative mode. As is well known, $[Ru(phen)_2(dppz)]^{2+}$ and $[Ru(bpy)_2(dppz)]^{2+}$ (phen = 1,10-phenanthroline, dppz = dipyrido-[3,2-*a*:2′,3′-*c*]phenazine, bpy = 2,2′-bipyridine) are

the most extensively investigated complexes as molecular 'light switches' for DNA; indeed, these complexes show no photoluminescence in aqueous solution at room temperature but display strong photoluminescence in DNA solution [5][8]. These excellent performances arise from the binding of the complexes to DNA in a typical interactive mode as well as from effective spectral properties. Therefore, continuously developing or modifying the intercalative ligand dppz is a very significative and promising work. Recently, a series of derivatives of $[Ru(L)_2(dppz)]^{2+}$ (L = bpy, phen), the parent complexes, have been synthesized through modifying the intercalative ligand (dppz), with the aim to improve the luminescence properties of the complexes as molecular 'light switches' for DNA [9–11]. More recently, *Ozawa et al.* reported the syntheses and luminescent behavior of $[Ru(bpy)_2L]^{2+}$ (L = dapq and pdpq; dapq = 2,4-diaminopyrimido[5,6-*b*]dipyrido[2,3-*f*:2′,3′-*h*]quinoxaline[1]), pdpq = 2,4(1*H*,3*H*)-pyrimidinedion[5,6-*b*]dipyrido[2,3-*f*:2′,3′-*h*]quinoxaline[1])) [12]. However, the DNA-binding properties of these complexes have not yet been reported. In particular, for further improved complexes of the type $[Ru(phen)_2L]^{2+}$, neither the DNA-binding property nor the luminescent behavior have been studied.

The [Ru^{II}(polypyridine)] complexes have also attracted the interest of many theoretical chemists. More and more computations, especially those applying the density-functional-theory (DFT) [13–16] and the time-dependent density-functional-theory (TDDFT) method [17][18] to Ru^{II} complexes, have been reported [19–21]. Furthermore, TDDFT can suit the calculations of the spectral properties of this type of complexes. We have also reported some DFT results on the electronic structures and related properties of some [Ru^{II}(polypyridine)] complexes [22–27]. Such theoretical studies on the electronic structures of complexes help to understand the trend of their DNA binding and related properties, thus guiding the design of suitable molecular modifications.

To further develop Ru^{II} complexes as DNA-'light switches', the DNA-binding and spectral properties of $[Ru(bpy)_2(ppn)]^{2+}$ (**1**) and further improved $[Ru(phen)_2(ppn)]^{2+}$ (**2**) are now studied in detail. These two complexes have excellent DNA-binding and optical properties, and thus they may become novel prospective DNA-'light switch' complexes. In particular, the DNA-'light switch' performance of complex **2** is superior to that of complex **1**. To better understand the DNA-binding and spectral behaviors of these complexes, DFT and TDDFT calculations were also carried out.

2. Results and Discussion. – 2.1. *Synthesis and Characterization.* The complexes **1**[2]) and **2**[2]) were prepared in moderate yields by direct reaction of the ligand ppn with a mol-equiv. of the precursor complex $[Ru(bpy)_2Cl_2]\cdot 2H_2O$ or $[Ru(phen)_2Cl_2]\cdot 2H_2O$ in EtOH/H_2O, respectively (*Scheme*). The complexes **1** and **2** were isolated as their perchlorates and purified by column chromatography. In the ES-MS of these perchlorates, only the signals of $[M - ClO_4^-]^+$ and $[M - 2ClO_4^-]^{2+}$ are observed. The

---

[1]) The abbreviations dapq and pdpq are based on these incorrect names. Thus the systematic name of dapq is pteridino[6,7-*f*][1,10]phenanthroline-11,13-diamine for which we use the abbreviation ppn. The systematic name of pdpq is pteridino[6,7-*f*][1,10]phenanthroline-11,13(10*H*,12*H*)-dione (ppd).

[2]) Arbitrary atom numbering; for systematic names, see *Exper. Part.*

measured relative molecular masses are consistent with the expected values. The ruthenium(II) complexes **1** and **2** give well-defined ^{1}H-NMR spectra ($(CD_3)_2SO$; *cf. Exper. Part*[3]). The δ(H) are assigned by comparison with those of similar compounds [28][29].

Scheme. *Preparation of the Ruthenium(II) Complexes* **1** *and* **2**

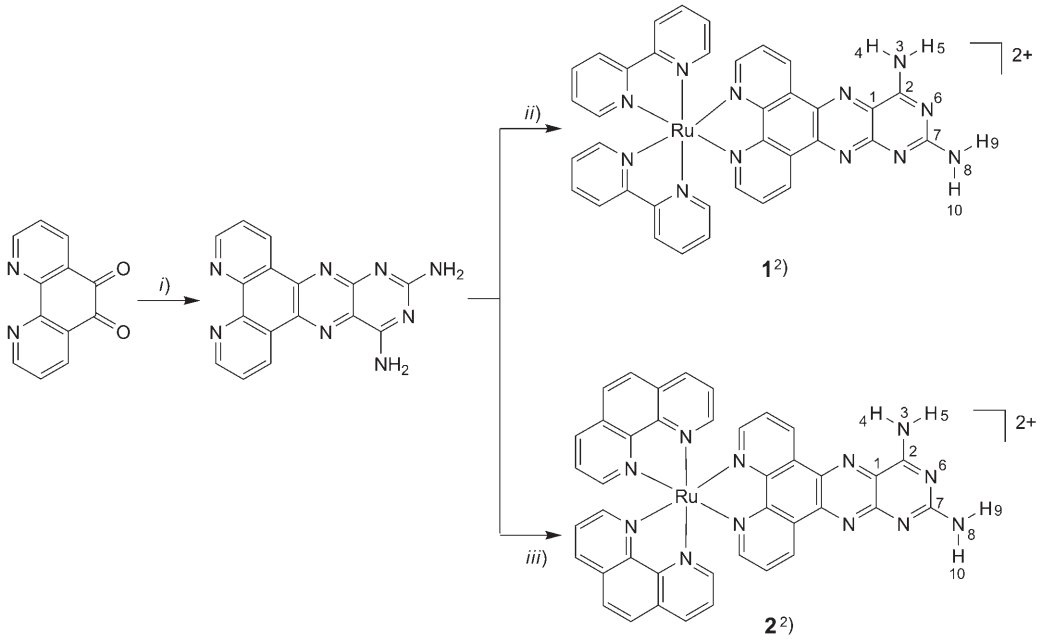

i) pyrimidine-2,4,5,6-tetramine sulfate + Na_2CO_3. *ii*) [Ru(bpy)$_2$Cl$_2$]. *iii*) [Ru(phen)$_2$Cl$_2$].

2.2. *Electrochemical Studies.* The electrochemical behaviors of the complexes were studied in MeCN by cyclic voltammetry. Both complexes exhibit well-defined waves in the sweep range from -2.0 to 1.8 V, *i.e.*, one oxidation and three reduction waves in the sweep range from -1.85 to $+1.70$ V, with half-wave potentials of $+1.33$, -1.0, -1.39, and -1.58 V *vs.* SCE for complex **1**, and $+1.34$, -0.97, -1.36, and -1.68 V for complex **2** (*Table 1*). The electrochemical behavior of [Ru^{II}(polypyridine)] complex is rationalized in terms of a metal-based oxidation and a series of reductions which are ligand-based, occur in stepwise manner, and are attributed to each π^* system. As expected, the oxidation potentials of **1** and **2** are more positive than those of $[Ru(bpy)_3]^{2+}$ and $[Ru(phen)_3]^{2+}$ due to the extension of the corresponding π framework. Moreover, the first reduction, which usually involves the ligand having the most stable lowest unoccupied molecular orbital (LUMO) [30], is assigned to a reduction centered on the ligand ppn, whereas the second and the third reductions are charac-

[3]) Supplementary material is available from the author *K.-C. Z.*

Table 1. *Electrochemical Data of the Ru^{II} Complexes in MeCN*[a])

	$E_{1/2ox}$ [V]	$E_{1/2red}$ [V]		
		I	II	III
$[Ru(bpy)_2(ppn)]^{2+}$ (**1**)	1.33	– 1.0	– 1.39	– 1.58
$[Ru(phen)_2(ppn)]^{2+}$ (**2**)	1.34	– 0.97	– 1.36	– 1.68
$[Ru(bpy)_3]^{2+}$ [47]	1.27	– 1.31	– 1.50	– 1.77
$[Ru(phen)_3]^{2+}$ [47]	1.27	– 1.35	– 1.52	–

[a]) All complexes were measured in 0.1M $(Bu_4N)ClO_4$ in MeCN *vs.* SCE, scan rate 100 $mV \cdot s^{-1}$.

teristic of the co-ligand bpy or phen [31]. Comparing the two Ru^{II} complexes, the oxidation potential of complex **2** shifts to a more positive value, suggesting that the co-ligand phen can better stabilize the Ru^{II} state than bpy, due to the greater extension of its π framework.

2.3. *Electronic Absorption Spectra.* Complex binding to DNA in the intercalation mode usually results in hypochromism and bathochromism in the absorption spectra, due to a strong $\pi-\pi$ stacking interaction between an aromatic chromophore and the base pairs of DNA. The extent of the hypochromism is closely related to the intercalative binding strength.

The absorption spectra of the two complexes **1** and **2** in the absence and presence of calf-thymus (CT) DNA at a constant complex concentration (20 μM) are given in *Fig. 1*. With increasing DNA concentration, the intense hypochromism and obvious red shift in the metal-to-ligand charge-transfer (MLCT) band of the complexes are observed. When the amount of DNA is increased, the hypochromism in the MLCT band of **1** at 431 nm is as high as 23.8%, with a red shift of 12 nm at a ratio [DNA]/[Ru] of 6.4, whereas the MLCT band of **2** at 431 nm exhibits hypochromism of *ca.* 24.8% with a red shift of 10 nm at a ratio [DNA]/[Ru] of 5.3. The hypochromism of **2** is much larger than that of **1**. These spectral characteristics suggest that both **1** and **2** most likely bind to DNA in the intercalative mode involving a strong stacking interaction between the aromatic chromophore (ppn) and the base pairs of the DNA.

To compare quantitatively the DNA-binding affinities of the two complexes **1** and **2**, the intrinsic binding constants K_b of the two complexes to DNA were obtained by monitoring the changes of the MLCT absorbance at 431 nm for both complexes according to *Eqns. 1* and *2* [10][33][34], where ε_a is the extinction coefficient observed for the MLCT absorption band at a given DNA concentration, ε_f is the extinction coefficient of the complex in the absence of DNA, ε_b is the extinction coefficient of the complex fully bound to DNA (when further addition of DNA does not change the absorbance, it is assumed that all complex molecules are bound to DNA, and ε_b can be calculated from *Beer*'s law). K_b is the equilibrium binding constant in M^{-1}, C_t is the total metal-complex concentration, [DNA] is the concentration of DNA in M (nucleotides), and s is the binding size.

$$(\varepsilon_a - \varepsilon_f)/(\varepsilon_b - \varepsilon_f) = (b - (b^2 - 2K_b^2 C_t[\mathrm{DNA}]/s)^{1/2})/2K_b C_t \quad (1)$$

$$b = 1 + K_b C_t + K_b[\mathrm{DNA}]/2s \quad (2)$$

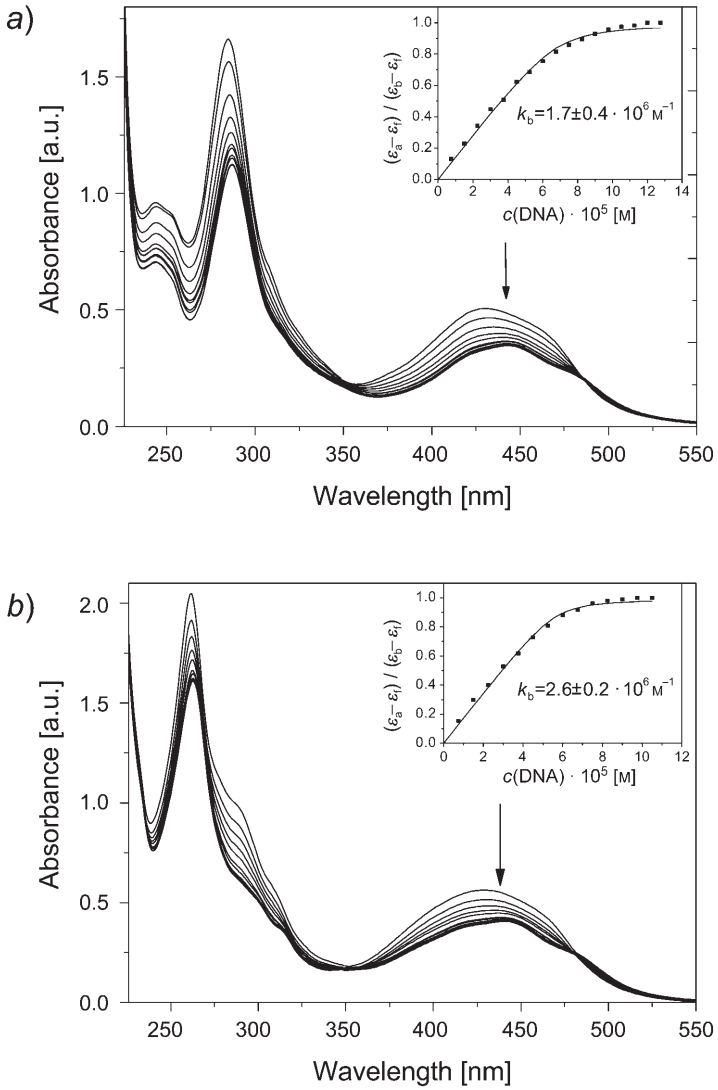

Fig. 1. *Absorption spectra of* a) *complex* **1** *and* b) *complex* **2** *in* Tris · *HCl buffer upon the addition of CT-DNA* ([Ru] = 20 μM, [DNA] = 0–130 μM). The arrows show the absorbance changes upon the increase of DNA concentration. Inset: plots of $(\varepsilon_a - \varepsilon_f)/(\varepsilon_b - \varepsilon_f)$ *vs.* [DNA] for the titration of the Ru^{II} complex by DNA (*cf. Eqns. 1* and *2*).

The experimental absorption–titration data were fitted to obtain the binding constants by a nonlinear least-squares method. The intrinsic binding constants K_b of complexes **1** and **2** were measured to be $(1.7 \pm 0.4) \cdot 10^6$ M^{-1} ($s = 1.71$) and $(2.6 \pm 0.2) \cdot 10^6$ M^{-1} ($s = 1.42$), respectively. These values are higher than those of the so-called DNA–intercalative Ru^{II} complexes ($1.1 \cdot 10^4 - 4.8 \cdot 10^4$ M^{-1}), but still slightly smaller than that of the parent complex $[Ru(phen)_2(dppz)]^{2+}$ ($K_b = 5.1 \cdot 10^6$ M^{-1} [35]).

Complex **2** exhibits a stronger DNA-binding affinity than complex **1**. The trend in the DNA-binding affinities and the spectral properties of **1** and **2** will be discussed in more detail in *Sect. 2.8* and *2.9*, respectively.

2.4. *Emission Spectra.* In the absence of DNA, complexes **1** and **2** show negligible luminescence in *Tris*·HCl buffer at room temperature, with a small maximum at 609 and 610 nm, and complex **2** exhibits a better molecular 'light switch' quality for DNA than complex **1** (see *Fig. 2*). Indeed, upon addition of CT-DNA, the emission intensity increases steadily to *ca.* 21.8 times of the original one in the case of **1** and to 73.5 times of the original one in the case of **2** (*Fig. 2*), establishing for both an obvious light-switch behavior. This implies that the two complexes can interact with CT-DNA and be efficiently protected by DNA since the hydrophobic environment inside the DNA helix reduces the accessibility of solvent water molecules to the complex, and the complex mobility is restricted at the binding site, leading to a decrease of the vibrational modes of relaxation.

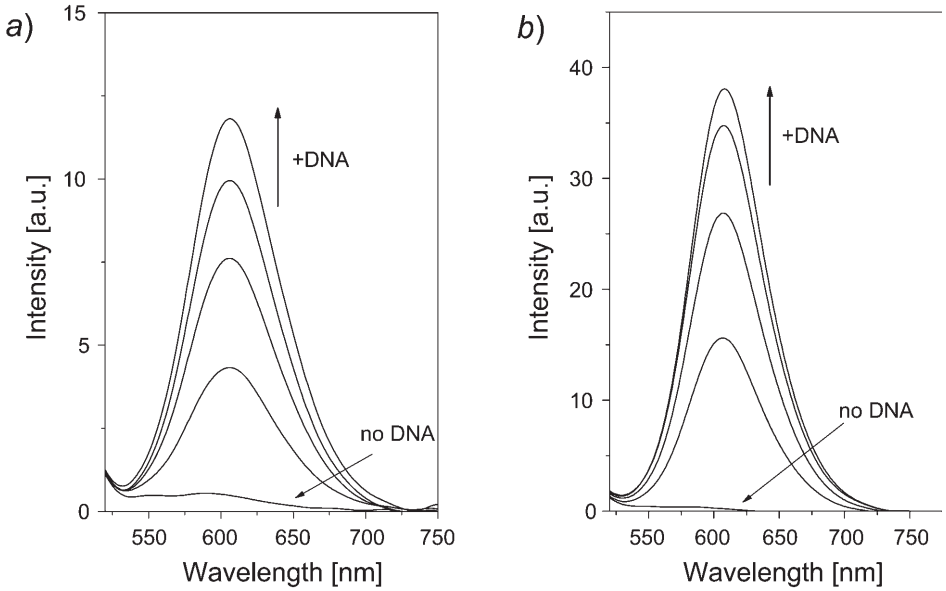

Fig. 2. *Emission spectra of* a*) complex* **1** *and* b*) complex* **2** (2 μM) *in* Tris·*HCl buffer at 298 K in the absence and presence of CT-DNA.* The arrows show the intensity change upon increasing DNA concentrations. Samples were excited at 440 nm; emission spectra were monitored between 500 and 750 nm.

2.5. *Steady-State Emission Quenching.* Steady-state emission-quenching experiments with $[Fe(CN)_6]^{4-}$ as quencher may provide further information about the binding of the complexes **1** and **2** to DNA. As illustrated in *Fig. 3*, in the presence of DNA, the emission intensity of the two complexes is hardly affected by the addition of anionic quencher, and the slope for complex **1** is larger than that for complex **2**. This may be explained by the repulsion of the highly negative $[Fe(CN)_6]^{4-}$ from the DNA polyanion backbone which hinders the access of $[Fe(CN)_6]^{4-}$ to the DNA-bound

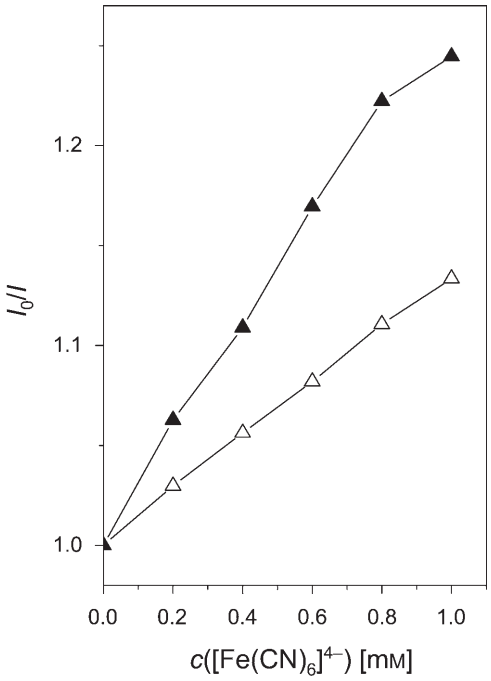

Fig. 3. *Emission quenching with* $[Fe(CN)_6]^{4-}$ *for* $[Ru(bpy)_2(ppn)]^{2+}$ (**1**; ▲) *and* $[Ru(phen)_2(ppn)]^{2+}$ (**2**; △) *in* Tris·*HCl buffer in the presence of CT-DNA.* [Ru] = 2 μM, [DNA]/[Ru] = 40.

complexes [36]. The curvature reflects the different extent of protection, a larger slope for the *Stern–Volmer* curve parallels poorer protection and lower binding. From *Fig. 3*, we can see that complex **2** binds stronger to DNA than complex **1**.

2.6. *Viscosity Studies.* To further elucidate the binding mode of complexes **1** and **2**, viscosity measurements of CT-DNA were carried out by varying the concentration of the added complexes. In fact, photophysical probes generally provide necessary but not sufficient clues to support a binding mode. Viscosity measurements, which are sensitive to DNA-length change, are regarded as the least ambiguous and the most critical tests of binding mode in solution in the absence of crystallographic structural data [37]. It is generally accepted that a classical intercalative mode results in lengthening the DNA helix, as base pairs are separated to accommodate the binding ligand, leading to the increase of DNA viscosity. In contrast, a partial and/or nonclassical intercalation of ligand could bend (or kink) the DNA helix, and thus reduce its effective length and, concomitantly, its viscosity [37].

The effects of complexes **1**, **2**, and $[Ru(bpy)_3]^{2+}$ on the viscosity of rod-like DNA show that complex $[Ru(bpy)_3]^{2+}$, which has been known to bind to DNA in an electrostatic mode, exerts essentially no effect on DNA viscosity (*Fig. 4*). When the amount of complexes **1** and **2** is increased, the relative viscosity of DNA increases steadily. The increase of viscosity, which may depend on the DNA-binding mode, follows the order of $\eta(\mathbf{2}) > \eta(\mathbf{1}) > \eta$ ($[Ru(bpy)_3]^{2+}$). The experimental results suggest that the two complexes bind to DNA in a classical intercalation mode. Due to the greater hydrophobic ability of the co-ligand phen, complex **2** can intercalate between

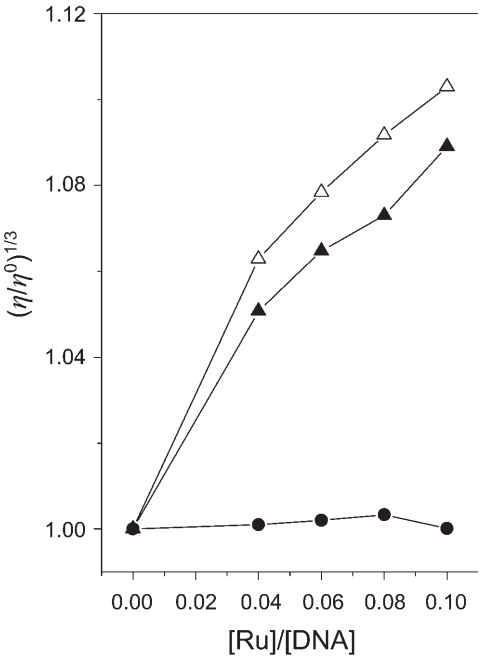

Fig. 4. *Effect of increasing amounts of complex* **1** (▲), *complex* **2** (△), *and* $[Ru(bpy)_3]^{2+}$ (●) *on the relative viscosity of DNA at* $30.0 \pm 0.1°$ *in* Tris · *HCl buffer.* [DNA] = 0.25 mM.

DNA base pairs deeply and show stronger DNA-binding affinity than complex **1** [23]. This is also consistent with the above spectroscopic results.

2.7. *Enantioselective Binding.* The equilibrium dialysis experiment may be one of the most direct means of examining the enantioselectivity of the complex binding to DNA. According to the DNA-binding model, the Δ-enantiomer binds preferentially to the right-handed helix [38]. The circular dichroism (CD) spectra in the UV region of complexes **1** and **2**, after dialysis of their racemic solutions against CT-DNA for 48 h, show strong CD signals, in the case of **1** with a negative peak at 276 nm and a positive peak at 293 nm, and in the case of **2** with a negative peak at 256 nm and a positive peak at 268 nm (*Fig. 5*). The control experiments show that no obvious CD signals are observed (data not presented). Although complexes **1** and **2** were both not resolved into their pure enantiomers, and we cannot experimentally determine which enantiomer of **1** and **2** binds to DNA enantioselectively, it is certain that **1** and **2** interact with CT-DNA enantioselectively.

2.8. *Theoretical Explanation of DNA-Binding Behaviors.* The different DNA-binding behaviors of the two complexes **1** and **2** can be reasonably explained by our theoretical computations with the DFT method and the frontier-molecular-orbital theory [39]. For comparison, the classical intercalator $[Ru(phen)_2(dppz)]^{2+}$ was also calculated with the same method. The cartesian coordinates of optimized geometries of these complexes can be obtained from the authors[3]) and some frontier-molecular-orbital (MO) energies are listed in *Table 2*. The MO contour maps are presented in *Fig. 6*.

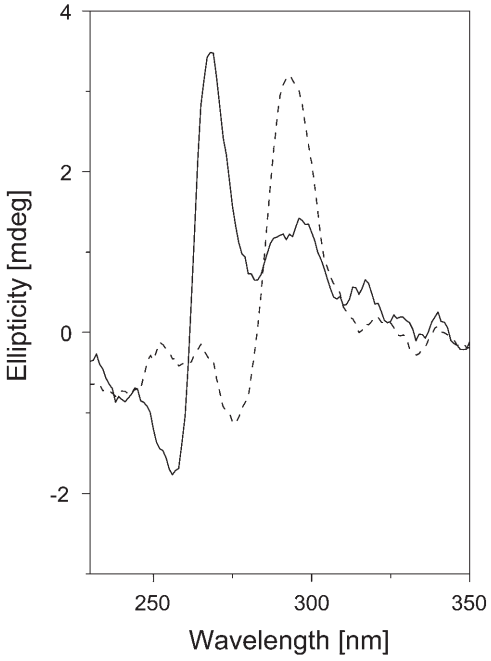

Fig. 5. *CD Spectra of the dialyzates of complex* **1** (----) *and complex* **2** (—) *in the presence of CT-DNA after 48 h dialysis of the stirred solution in* Tris·*HCl buffer*. [Ru] = 20 μM, [DNA] = 0.5 mM.

Table 2. *Some Frontier-Molecular-Orbital Energies* (ε_i [a.u.]) *and Related Energy Differences* ($\Delta\varepsilon$) *of Complexes* **1**, **2**, *and [Ru(phen)$_2$(dppz)]$^{2+}$* (1 a.u. = 27.21 eV)

	H-2	H-1	HOMO[a])	LUMO[b])	L+1	L+2	L+3	$\Delta\varepsilon_{L-H}$[c])
1	−0.3974	−0.3848	−0.3756	−0.2742	−0.2709	−0.2660	−0.2588	0.1106
2	−0.3940	−0.3828	−0.3735	−0.2683	−0.2648	−0.2631	−0.2614	0.1145
[Ru(phen)$_2$(dppz)]$^{2+}$	−0.3999	−0.3973	−0.3961	−0.2702	−0.2667	−0.2665	−0.2630	0.1271

[a]) HOMO (or H): the highest occupied molecular orbital; H-1: the next HOMO. [b]) LUMO (or L): the lowest unoccupied molecular orbital; L+1: the next LUMO. [c]) $\Delta\varepsilon_{L-H}$: energy difference between LUMO and HOMO.

As is well-established, there are π–π stacking interactions upon DNA binding of complexes such as **1** or **2** in the intercalation (or partial intercalation) mode [28], and many theoretical studies [40] have shown that the DNA molecule is an electron donor and the intercalated complex is an electron acceptor. Therefore, the factors affecting DNA-binding affinities of the complex can usually be evaluated from the planarity and plane area of an intercalative ligand and from the energy and population of the lowest unoccupied molecular orbital (LUMO, even and LUMO + x) of the complex molecule. The lower LUMO (and LUMO + x) of the complex easily accepts electrons from the HOMO (and HOMO − x) of DNA base pairs, and the increased population of LUMO (and LUMO + x) on the intercalative ligand is advantageous to the orbital interaction

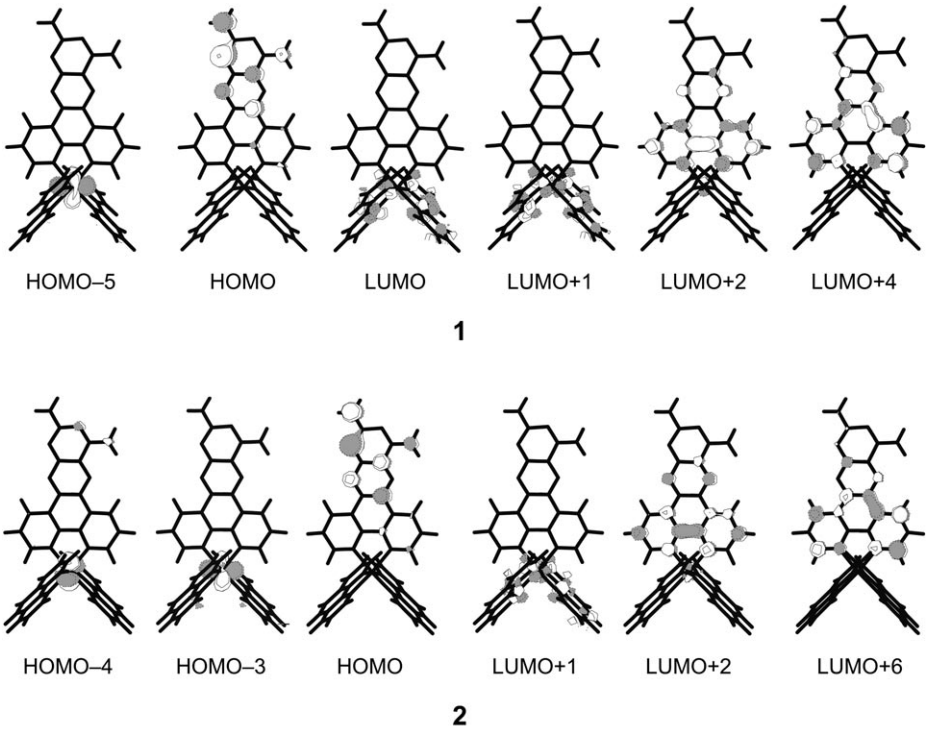

Fig. 6. *Some related frontier-MO contour maps of complexes [Ru(L)$_2$(ppn)]$^{2+}$* **1** *and* **2** (L = bpy and phen, resp.) *calculated with the DFT method at the B3LYP/LanL2DZ level.* The corresponding frontier-MO contour maps of [Ru(phen)$_2$(dppz)]$^{2+}$ can be obtained from the authors[3]).

between the LUMO (and LUMO + x) of the complex and the HOMO (and HOMO − x) of DNA according to the frontier molecular orbital theory [39].

From *Table 3* we can see that the intercalative ligand of complexes **1** and **2** still retains an excellent conjugative planarity and a quite extended planar area, like the parent complex [Ru(phen)$_2$(dppz)]$^{2+}$. So they can deeply be inserted into DNA by the intercalation mode and exhibit large DNA-binding constants. Furthermore, from *Fig. 6*, we can see that the related frontier-MO contour maps of these two complexes are very alike, their LUMO + x ($x = 2$ and so on) are distributed on the intercalative ligand, and thus their LUMO + x ($x = 2$ and so on) should play an important role in accepting electrons from base pairs of DNA. For comparison, the frontier-MO contour maps of complex [Ru(phen)$_2$(dppz)]$^{2+}$ show that its LUMO + x ($x = 1$ and so on) are distributed on the intercalative ligand (contour maps available from the authors[3])).

The experimental results established the following trend in the DNA-binding constants (K_b): $K_b([Ru(phen)_2(dppz)]^{2+}) > K_b(\mathbf{2}) > K_b(\mathbf{1})$. The fact that $K_b([Ru(phen)_2(dppz)]^{2+}) > K_b(\mathbf{2})$ can be attributed to the order of the energies of the LUMO + x ($x = 0$, 1, 2) of complexes **2** and [Ru(phen)$_2$(dppz)]$^{2+}$ which are all $\varepsilon_{LUMO+x}(\mathbf{2}) > \varepsilon_{LUMO+x}([Ru(phen)_2(dppz)]^{2+})$ and to some LUMO + x being distributed on the intercalative ligands. The fact that $K_b(\mathbf{2}) > K_b(\mathbf{1})$ can be attributed to the larger

Table 3. *Computed Selective Bond Lengths, Bond Angles, and Dihedral Angles of Complexes* $[Ru(bpy)_2(ppn)]^{2+}$ (**1**) *and* $[Ru(phen)_2(ppn)]^{2+}$ (**2**)

	1	**2**
$Ru-N_m$[a]) [nm]	0.2109	0.2106
$N-Ru-N_m$ [°]	79.2	79.3
$C-C(C-N)_m$[b]) [nm]	0.1398	0.1399
$Ru-N_{co}$ [nm][a])	0.2097	0.2106
$N-Ru-N_{co}$ [°]	78.5	79.5
$C-C(C-N)_{co}$ [nm]	0.1400	0.1405
C(1)–C(2)–N(3)–H(4) [°][2])	0.02	0.07
C(1)–C(2)–N(3)–H(5) [°][2])	179.9	180.0
N(6)–C(7)–N(8)–H(9) [°][2])	0.01	−0.01
N(6)–C(7)–N(8)–H(10) [°][2])	−179.9	179.9

[a]) $Ru-N_m$ = mean bond length between Ru and the coordinating N-atoms of the main ppn ligand; $Ru-N_{co}$ = mean bond length between Ru and the coordinating N-atoms of the co-ligand. [b]) $C-C(C-N)_m$ = the mean bond length of the ppn skeleton.

hydrophobicity of the ancillary ligand phen compared to that of bpy. Since a larger hydrophobicity allows the main ligand ppn a more efficient intercalation between the base-pairs of DNA thus renders its interaction with the base-pairs of DNA stronger. This result is in agreement with our previous work [23].

2.9. *Theoretical Explanation of the Electronic-Absorption Spectral Properties.* Since the ^{1}MLCT band in the absorption spectra plays a very important role in the study of the interaction between a complex and DNA, the details of these spectra were analyzed theoretically by the TDDFT approach. The calculated wavelengths λ in the range 400–500 nm, *i.e.*, the bands with ^{1}MLCT properties, the oscillator strengths ($f \geq 0.07$), and the main orbital-transition contributions ($\geq 15\%$) of complexes **1** and **2** in the gas phase, calculated with the TDDFT at the level of B3LYP/LanL2DZ, as well as the experimental λ values, are given in *Table 4* and compared with those of the classical intercalator $[Ru(phen)_2(dppz)]^{2+}$. For complex **1**, three transitions with $f > 0.07$ lie in the range 400–500 nm. Among them, the two transitions at 438.9 ($f = 0.099$) and 424.7 ($f = 0.173$) have obvious ^{1}MLCT character and mainly originate from $d_{Ru} \rightarrow \pi^*_{bpy}$ transitions; therefore, the experimental stronger and wider band at 431 nm can be assigned to the superposition of these two bands with ^{1}MLCT character. The strong transition at 410.3 nm ($f = 0.156$) with ^{1}LL (ligand-to-ligand) character arises mainly from the $\pi \rightarrow \pi^*$ transition of the intercalative ligand ppn. A similar analysis can be applied to complex **2**. However, different from **1**, there are two transitions at 420.3 ($f = 0.140$) and at 404.5 nm ($f = 0.082$) with ^{1}MLCT character, their superposition explains the experimental band at 431 nm. Again a strong transition with ^{1}LL character at 407.5 nm ($f = 0.239$) arises from the $\pi_L \rightarrow \pi^*_L$ transition. In the case of $[Ru(phen)_2(dppz)]^{2+}$, the experimental stronger and wider band at 439 nm can be assigned to the superposition of two bands with ^{1}MLCT character, *i.e.*, those at 426.2 nm ($f = 0.168$) and 405.3 nm ($f = 0.10$).

Table 4. *Calculated and Experimental Wavelengths* (λ_{max}) *as well as Oscillator Strengths* ($f \geq 0.07$) *and Main Orbital-Transition Contributions* ($\geq 15\%$) *of the Absorption Spectra of* $[Ru(bpy)_2(ppn)]^{2+}$ (**1**), $[Ru(phen)_2(ppn)]^{2+}$ (**2**), *and* $[Ru(phen)_2(dppz)]^{2+}$, *Calculated with TDDFT at the Level of B3LYP/LanL2DZ in the Gas Phase*

	λ_{max} [nm]		f	Assignment	Character
	exper.[a])	calc.[b])			
1	431	438.9	0.099	HOMO-5 → LUMO(64%) $d_{Ru} \rightarrow \pi^*_{bpy}$	^{1}MLCT
		424.7	0.173	HOMO-5 → LUMO + 1(51%) $d_{Ru} \rightarrow \pi^*_{bpy}$	^{1}MLCT
		410.3	0.156	HOMO → LUMO + 4(66%) $\pi_L \rightarrow \pi^*_L$	^{1}LL
2	431	420.3	0.140	HOMO-4 → LUMO + 2(37%) $d_{Ru} \rightarrow \pi^*_L$	
				HOMO-3 → LUMO + 1(15%) $d_{Ru} \rightarrow \pi^*_{phen}$	^{1}MLCT
		407.5	0.239	HOMO → LUMO + 6(63%) $\pi_L \rightarrow \pi^*_L$	^{1}LL
		404.5	0.082	HOMO-4 → LUMO + 3(59%) $d_{Ru} \rightarrow \pi^*_{phen}$	^{1}MLCT
$[Ru(phen)_2(dppz)]^{2+}$	439	426.2	0.168	HOMO-2 → LUMO + 1(50%) $d_{Ru} \rightarrow \pi^*_{dppz}$	^{1}MLCT
		405.3	0.100	HOMO-2 → LUMO + 3(67%) $d_{Ru} \rightarrow \pi^*_{phen}$	^{1}MLCT

[a]) In aqueous solution. [b]) In the gas phase.

An analogous theoretical analysis of the corresponding absorption spectra in aqueous solution does not provide a substantial improvement compared to the gas-phase analysis[3]).

3. Conclusions. – In summary, the two Ru^{II} complexes $[Ru(bpy)_2(pn)]$ (**1**) and $[Ru(phen)_2(ppn)]$ (**2**) do not (or negligibly) exhibit background emission in aqueous solution because their ligand ppn contains four N-atoms with lone-pair electrons which can strongly interact with H_2O molecules, thus leading to the luminescence inactivity. However, in the presence of DNA, the ligand ppn of **1** and **2** can bind to the base-pairs of DNA in an intercalative mode, and these N-atoms of ppn can be efficiently protected by DNA from their interaction with H_2O, and thus the excited Ru^{II} complexes show strong luminescence. In addition, the lowest-energy electron absorption spectra of **1** and **2** possess the typical ^{1}MLCT character with higher strength, and the corresponding emission spectra (luminescence) usually possess the same character as well. Therefore, complex **1**, and especially complex **2**, can be expected to be DNA-'light switch' complexes. The DNA-binding constants K_b are quite large, *i.e.*, $K_b(\mathbf{1}) = (1.7 \pm 0.4) \cdot 10^6$ M^{-1} and $K_b(\mathbf{2}) = (2.6 \pm 0.2) \cdot 10^6$ M^{-1}. The experimental results further establish that the ancillary ligands not only have a significant effect on the DNA-binding affinity of the complex but also have a certain effect on the spectral properties of the complexes, *i.e.*, $[Ru(phen)_2(dapq)]^{2+}$(**2**) has a better DNA-binding and luminescent behavior than $[Ru(bpy)_2(dapq)]^{2+}$(**1**), suggesting that $[Ru(phen)_2(dapq)]^{2+}$(**2**) might be a more prospective DNA-'light switch' complex. To understand these experimental results, the DFT/TDDFT computations offered some useful theoretical confirmations of the DNA binding as well as of the spectral properties of these complexes.

We are grateful to the supports of the *National Natural Science Foundation of China*, the *Research Fund for the Doctoral Program of Higher Education*, and the *Natural Science Foundation of Guangdong Province of China.*

Experimental Part

1. *General.* All reagents and solvents were commercially available and used without further purification unless otherwise noted. The dialysis membrane was purchased from *Union Carbide Co.* and treated by means of a general procedure before use [41]. Solns. of CT-DNA in 50 mM NaCl/5 mM *Tris*·HCl (tris(hydroxymethyl)aminomethane hydrochloride = 2-amino-2-(hydroxymethyl)propane-1,3-diol), pH 7.2 gave a ratio of UV/VIS absorbance of 1.8–1.9 : 1 at 260 and 280 nm, indicating that the DNA was sufficiently free of protein [42]. The concentration of DNA was determined spectrophotometrically by using a molar absorptivity of 6600 $M^{-1}cm^{-1}$ (260 nm) [43]. Double-distilled H_2O was used to prepare buffers.

2. *Bis(2,2′-bipyridine-*κN^{1},$\kappa N^{1'}$*)(pteridino[6,7-f][1,10]phenanthroline-11,13-diamine-*κN^{3},κN^{5}*)ruthenium(2+) Perchlorate (1:2)* (**1**) *and Bis(1,10-phenanthroline-*κN^{1},κN^{10}*)(pteridino[6,7-f][1,10]phenanthroline-11,13-diamine-*κN^{3},κN^{5}*)ruthenium(2+) Perchlorate (1:2)* (**2**). The compounds *cis*-$[Ru(bpy)_2Cl_2]\cdot 2H_2O$, *cis*-$[Ru(phen)_2Cl_2]\cdot 2H_2O$, and 1,10-phenanthroline-5,6-dione (= phendione) were prepared by the literature methods [44]. The ligand ppn, $[Ru(bpy)_2(ppn)](ClO_4)_2$ (**1**), and $[Ru(phen)_2(ppn)](ClO_4)_2$ (**2**) were also synthesized by the literature method [12]. *Caution:* Perchlorate complexes are potential explosives and must be handled in small quantity and with great care. ^{1}H-NMR ($(CD_3)_2SO$; **1**): *Fig. S1*, *top*[3]). ^{1}H-NMR ($(CD_3)_2SO$; **2**): *Fig. S1*, *bottom*[3]). Absorption spectra: *Perkin-Elmer-Lambda850* spectrophotometer. Emission spectra: *Perkin-Elmer Ls55* spectrofluorophotometer; at r.t. Cyclic voltammetry: *EG&G-PAR-273* polarographic analyzer and *270* universal programmer; supporting electrolyte, 0.1 M $(Bu_4N)ClO_4$ in MeCN (freshly distilled from P_2O_5 and deaerated by purging with N_2); standard three-electrode system comprising a Pt-microcylinder working electrode, a Pt-wire auxiliary electrode, and a sat. calomel reference electrode (SCE). ^{1}H-NMR Spectra: *Varian Inova-500* spectrometers; in $(CD_3)_2SO$ at r.t., $SiMe_4$ as the internal standard[3]). Electrospray (ES) MS: *LQC* system (*Finngan MAT*, USA), MeCN as mobile phase; spray voltage, tube lens offset, capillary voltage, and capillary temp. at 4.50 KV, 30.00 V, 23.00 V, and 200 °C, resp. Microanalyses (C, H, and N): *Perkin-Elmer 240Q* elemental analyzer.

3. *DNA-Binding Experiments. Absorption Titrations.* The titrations of Ru^{II} complexes **1** or **2** in buffer (5 mM *Tris*·HCl, 50 mM NaCl, pH 7.2) were performed by using a fixed Ru^{II} concentration to which increments of a DNA stock soln. were added. The employed concentrations of the Ru^{II} solns. were 20 μM, and CT-DNA was added to achieve a ratio [DNA]/[Ru] of 7.5 : 1. Ru^{II}/DNA Solns. were allowed to incubate for 10 min before the absorption spectra were recorded.

Viscosity Measurements. A *Ubbelohde* viscometer was maintained at a constant temp. of 30.0 ± 0.1° (thermostatic bath). The flow time was measured with a digital stopwatch. Every sample was measured three times, and an average flow time was calculated. Data are presented as $(\eta/\eta^0)^{1/3}$ *vs.* the binding ratio [45], where η is the viscosity of DNA in the presence of complex and η^0 is the viscosity of DNA alone.

Equilibrium Dialysis Measurements. The measurements were conducted at r.t. with 5 ml of CT-DNA (0.5 mM) sealed in a dialysis bag (cellulose membrane) and 10 ml of the Ru^{II} complex soln. (20 μM) outside the bag, with stirring of the soln. for 48 h. In the control experiments, 5 mol of *Tris*·HCl buffer was used instead of CT-DNA. Before use, the dialysis membranes were boiled for *ca.* 1 h in a 1% EDTA (ethylenediaminetetraacetic acid = *N*,*N*′-ethane-1,2-diylbis[*N*-(carboxymethyl)glycine]) and 3% $NaHCO_3$ soln. and then rinsed in doubly deionized H_2O.

4. *Theoretical Calculations.* Each complex **1** or **2** of the general structure $[Ru(L)_2(ppn)]^{2+}$ (L = bpy or phen) was formed from Ru^{II}, one ligand ppn, and two co-ligands (bpy or phen). There is no symmetry in these complexes. The full geometry optimization computations were performed with the DFT method [13–16] at the B3LYP/LanL2DZ [46] level for **1** and **2** in the ground-state with the singlet state [31]. The frequency calculations were also performed to verify that the optimized structure was at an energy minimum. Furthermore, the electronic absorption spectra in the gas phase and in aq. soln. were calculated by TDDFT at the B3LYP/LanL2DZ level, and 50 singlet-excited-state energies of each complex were calculated. The conductor polarizable continuum model (CPCM) [47] was applied to the solvent effect in aq. soln. To easily and clearly understand the related properties of the complexes, the schematic diagrams of some related frontier molecular orbitals (MO) of the complexes were drawn with the Molden v4.4 program [32] based on the DFT computational results. All computations were performed with the Gaussian 03 quantum chemistry program-package [48].

REFERENCES

[1] M. J. Clarke, *Coord. Chem. Rev.* **2003**, *236*, 209.
[2] L. N. Ji, X. H. Zou, J. G. Liu, *Coord. Chem. Rev.* **2001**, *216–217*, 513.
[3] M. K. Nazeeruddin, S. M. Zakeeruddin, R. Humphry-Baker, S. I. Gorelsky, A. B. P. Lever, M. Grätzel, *Coord. Chem. Rev.* **2000**, *208*, 213.
[4] M. F. Ottaviani, N. D. Ghatlia, S. H. Bossmann, J. K. Barton, H. Duerr, N. J. Turro, *J. Am. Chem. Soc.* **1992**, *114*, 8946.
[5] A. E. Friedman, J. C. Chambron, J. P. Sauvage, N. J. Turro, J. K. Barton, *J. Am. Chem. Soc.* **1990**, *112*, 4960.
[6] E. Ruba, J. R. Hart, J. K. Barton, *Inorg. Chem.* **2004**, *43*, 4570.
[7] P. Uma Maheswari, V. Rajendiran, H. Stoeckli-Evans, M. Palaniandavar, *Inorg. Chem.* **2006**, *45*, 37.
[8] R. M. Hartshorn, J. K. Barton, *J. Am. Chem. Soc.* **1992**, *114*, 5919.
[9] M. K. Brennaman, T. J. Meyer, J. M. Papanikolas, *J. Phys. Chem., A* **2004**, *108*, 9938.
[10] J. Olofsson, L. M. Wilhelmsson, P. Lincoln, *J. Am. Chem. Soc.* **2004**, *126*, 15458.
[11] F. Gao, H. Chao, F. Zhou, Y. X. Yuan, B. Peng, L. N. Ji, *J. Inorg. Biochem.* **2006**, *100*, 1487.
[12] T. Ozawa, Y. Kishi, K. Miyamoto, K. Wasada-Tsutsui, Y. Funahashi, K. Jitsukawa, H. Masuda, *Adv. Mater. Res.* **2006**, *11–12*, 277.
[13] J. B. Foresman, M. J. Frisch, in 'Exploring Chemistry with Electronic Structure Methods', 2nd edn., Gaussian Inc., Pittsburgh, 1996.
[14] P. Hohenberg, W. Kohn, *Phys. Rev. B: Condens. Matter* **1964**, *136*, 864.
[15] A. D. Becke, *J. Chem. Phys.* **1993**, *98*, 1372.
[16] A. Görling, *Phys. Rev. A: At., Mol., Opt. Phys.* **1996**, *54*, 3912.
[17] P. J. Hay, *J. Phys. Chem.*, *A* **2002**, *106*, 1634.
[18] G. Pourtois, D. Beljonne, C. Moucheron, S. Schumm, A. Kirsch-DeMesmaeker, R. Lazzaroni, J. L. Bredas, *J. Am. Chem. Soc.* **2004**, *126*, 683.
[19] S. R. Stoyanov, J. M. Villegas, D. P. Rillema, *Inorg. Chem.* **2002**, *41*, 2941.
[20] J. Li, L. C. Xu, J. C. Chen, K. C. Zheng, L. N. Ji, *J. Phys. Chem., A* **2006**, *110*, 8174.
[21] L. C. Xu, J. Li, Y. Shen, K. C. Zheng, L. N. Ji, *J. Phys. Chem., A* **2007**, *111*, 273.
[22] K. C. Zheng, J. P. Wang, Y. Shen, W. L. Peng, F. C. Yun, *J. Chem. Soc., Dalton Trans.* **2002**, 111.
[23] H. Xu, K. C. Zheng, H. Deng, L. J. Lin, Q. L. Zhang, L. N. Ji, *New J. Chem.* **2003**, *27*, 1255.
[24] S. Shi, J. Liu, J. Li, K. C. Zheng, C. P. Tan, L. M. Chen, L. N. Ji, *Dalton Trans.* **2005**, 2038.
[25] F. Gao, H. Chao, F. Zhou, L. C. Xu, K. C. Zheng, L. N. Ji, *Helv. Chim. Acta* **2007**, *90*, 36.
[26] X. W. Liu, J. Li, H. Deng, K. C. Zheng, Z. W. Mao, L. N. Ji, *Inorg. Chim. Acta* **2005**, *358*, 3311.
[27] X. W. Liu, J. Li, H. Li, K. C. Zheng, H. Chao, L. N. Ji, *J. Inorg. Biochem.* **2005**, *99*, 2372.
[28] X. H. Zou, B. H. Ye, H. Li, Q. L. Zhang, H. Chao, J. G. Liu, L. N. Ji, X. Y. Li, *J. Biol. Inorg. Chem.* **2001**, *6*, 143.
[29] A. Chouai, S. E. Wicke, C. Turro, J. Bacsa, K. R. Dunbar, D. Wang, R. P. Thummel, *Inorg. Chem.* **2005**, *44*, 5996.
[30] B. K. Ghosh, A. Chakra-Vorty, *Coord. Chem. Rev.* **1989**, *95*, 239.
[31] A. Juris, V. Balzani, F. Barigelletti, S. Campagna, P. Belser, A. von Zelewsky, *Coord. Chem. Rev.* **1988**, *84*, 85.
[32] G. Schaftenaar, J. H. Noordik, *J. Comput.-Aided Mol. Des.* **2000**, *14*, 123.
[33] S. R. Smith, G. A. Neyhart, W. A. Karlsbeck, H. H. Thorp, *New J. Chem.* **1994**, *18*, 397.
[34] M. T. Carter, M. Rodrigues, A. J. Bard, *J. Am. Chem. Soc.* **1989**, *111*, 8901.
[35] B. N. Rajesh, S. T. Emily, L. K. Shalawn, J. M. Catherine, *Inorg. Chem.* **1998**, *37*, 139.
[36] C. V. Kumar, N. J. Turro, J. K. Barton, *J. Am. Chem. Soc.* **1985**, *107*, 5518.
[37] S. Satyanarayana, J. C. Dabroniak, J. B. Chaires, *Biochemistry* **1992**, *31*, 9319; S. Satyanarayana, J. C. Daborusak, J. B. Chaires, *Biochemistry* **1993**, *32*, 2573; Y. J. Liu, H. Chao, J. H. Yao, H. Li, Y. X. Yuan, L. N. Ji, *Helv. Chim. Acta* **2004**, *87*, 3119.
[38] J. K. Barton, *Science (Washington, DC, U.S.)* **1986**, *233*, 727; A. Ambroise, B. G. Maiya, *Inorg. Chem.* **2000**, *39*, 4256.

[39] G. Klopman, *J. Am. Chem. Soc.* **1968**, *90*, 223; I. Fleming, 'Frontier Orbitals and Organic Chemical Reactions', Wiley, New York, 1976.
[40] N. Kurita, K. Kobayashi, *Comput. Chem.* **2000**, *24*, 351; D. Reha, M. Kabelac, F. Ryjacek, J. Sponer, J. E. Sponer, M. Elstner, S. Suhai, P. Hobza, *J. Am. Chem. Soc.* **2002**, *124*, 3366.
[41] J. K. Barton, J. J. Dannenberg, A. L. Raphael, *J. Am. Chem. Soc.* **1984**, *106*, 2172.
[42] J. Marmur, *J. Mol. Biol.* **1961**, *3*, 208.
[43] M. E. Reichmann, S. A. Rice, C. A. Thomas, P. Doty, *J. Am. Chem. Soc.* **1954**, *76*, 3047.
[44] B. P. Sullivan, D. J. Salmon, T. J. Meyer, *Inorg. Chem.* **1978**, *17*, 3334; M. Yamada, Y. Tanaka, Y. Yoshimato, S. Kuroda, I. Shimao, *Bull. Chem. Soc. Jpn.* **1992**, *65*, 1006.
[45] G. Cohen, H. Eisenberg, *Biopolymers* **1969**, *8*, 45.
[46] A. D. Becke, *J. Chem. Phys.* **1993**, *98*, 5648; C. Lee, W. Yang, R. G. Parr, *Phys. Rev. B: Condens. Matter* **1988**, *37*, 785; P. J. Hay, W. R. Wadt, *J. Chem. Phys.* **1985**, *82*, 270.
[47] V. Barone, M. Cossi, *J. Phys. Chem., A* **1998**, *102*, 1995; M. Cossi, N. Rega, G. Scalmani, V. Barone, *J. Comput. Chem.* **2003**, *24*, 669; J. Andzelm, C. Kölmel, A. Klamt, *J. Chem. Phys.* **1995**, *103*, 9312.
[48] M. J. Frisch, G. W. Trucks, H. B. Schlegel, G. E. Scuseria, M. A. Robb, J. R. Cheeseman, J. A. Montgomery Jr., T. Vreven, K. N. Kudin, J. C. Burant, J. M. Millam, S. S. Iyengar, J. Tomasi, V. Barone, B. Mennucci, M. Cossi, G. Scalmani, N. Rega, G. A. Petersson, H. Nakatsuji, M. Hada, M. Ehara, K. Toyota, R. Fukuda, J. Hasegawa, M. Ishida, T. Nakajima, Y. Honda, O. Kitao, H. Nakai, M. Klene, X. Li, J. E. Knox, H. P. Hratchian, J. B. Cross, V. Bakken, C. Adamo, J. Jaramillo, R. Gomperts, R. E. Stratmann, O. Yazyev, A. J. Austin, R. Cammi, C. Pomelli, J. W. Ochterski, P. Y. Ayala, K. Morokuma, G. A. Voth, P. Salvador, J. J. Dannenberg, V. G. Zakrzewski, S. Dapprich, A. D. Daniels, M. C. Strain, O. Farkas, D. K. Malick, A. D. Rabuck, K. Raghavachari, J. B. Foresman, J. V. Ortiz, Q. Cui, A. G. Baboul, S. Clifford, J. Cioslowski, B. B. Stefanov, G. Liu, A. Liashenko, P. Piskorz, I. Komaromi, R. L. Martin, D. J. Fox, T. Keith, M. A. Al-Laham, C. Y. Peng, A. Nanayakkara, M. Challacombe, P. M. W. Gill, B. Johnson, W. Chen, M. W. Wong, C. Gonzalez, J. A. Pople, Gaussian 03, Revision D.01, *Gaussian Inc.*, Wallingford CT, 2005.

Received January 2, 2008